Shaping vessels and microenvironment: adipose stromal cells in retinal-related diseases

Terlizzi, Vincenzo

Chapter 5

Adipose Tissue-derived Stromal/Stem Cells Movement, Organization and Vasculogenic Activity in Confined Three- Dimensional Microenvironments

Adipose tissue-derived stromal/stem cells movement, organization and vasculogenic activity in confined three- dimensional microenvironments

Vincenzo Terlizzi[1], Gabriel Romero Liguori[1,4], Janette Kay Burgess[3], Hans Peter Hammes[2], Martin Conrad Harmsen[1]

1. University of Groningen, University Medical Center Groningen, Department of Pathology and Medical Biology, Lab for Cardiovascular Regenerative Medicine (CAVAREM), Groningen, The Netherlands

2. 5th Medical Department, Section of Endocrinology, Medical Faculty Mannheim, University of Heidelberg, Germany

3. University of Groningen, University Medical Center Groningen, Department of Pathology and Medical Biology, GRIAC Research Institute, Groningen, The Netherlands

4. Heart Institute (InCor), Hospital das Clínicas da Faculdade de Medicina da Universidade de São Paulo, Laboratory of Cardiovascular Surgery and Circulation Pathophysiology (LIM-11)

In preparation

Abstract

Adipose tissue-derived stromal/stem cells (ASC) are multipotent cells that control connective tissue homeostasis in adipose tissue. In pathological conditions, such as diabetes, extracellular matrix and vascular network changes result in a pro-angiogenic turnover that alters the physiological state of the tissue. We hypothesized that ASC promotion of vascular network formation is induced by the combination of juxtacrine communication and extracellular matrix deposition. In this study, three-dimensional printed scaffolds were used to investigate ASC spatial distribution in regulating extracellular matrix and vessel tube formation *in vitro*. Coculturing ASC from healthy donors with human umbilical vein endothelial cells (HUVEC) and porcine microvascular endothelial cells (PREC) promoted interconnected endothelial cell tubes and homogeneous secretion of fibronectin. In contrast, ASC from diabetic patients did not promote tube formation, while fibronectin was not homogeneously secreted compare to the healthy ASC. ASC and endothelial cells assembly was further investigated using the combination of scaffolds, matrigel® and time-lapse confocal microscopy. Cocultured cells actively degraded matrigel® facilitating interconnected cavities of a diameter of ~20µm. ASC expression of F-actin and transgelin suggested ASC were motile. The cavities were exploited by HUVEC and PREC to enable formation of cellular aggregates. Cellular aggregates sprouted and connected as to form a vessel-like networks in 10 days. Long term cultures (over 23 days) retained the cells' movements. Endothelial cells surrounded by contractile ASC, protruded at differential speeds ranging from 2 to 20µm per hour. In conclusion, this approach showed that the combination of ASC and endothelial cells retains a high degree of heterogeneity. Degradation of the host matrigel® was followed by newly deposited extracellular matrix that promoted vessel-like network formation. Technically, three-dimensional printed scaffolds, matrigel® and time-lapse microscopy allow precise cellular process observation as well as providing new tools for studying diseases.

Introduction

In adipose tissue, adipose tissue-derived stromal/stem cells (ASC) [1,2] are adult multipotent cells that function as perivascular cells to contribute in tissue homeostasis and promote wound healing [3]. Adipose tissue angiogenesis and vascular maintenance are fundamental processes involved in the pathogenesis of diseases such as diabetes mellitus [4]. A variety of factors i.e. growth factors, cytokines and cells' metabolic changes modulate the surrounding tissues' microenvironment under pathological conditions, and promote abnormalities in the microcirculation [5]. ASC induce endothelial cells assembly in a vessel-like network through the production of extracellular matrix proteins which constitute a basement membrane (collagen, fibronectin, and laminin) indispensable for endothelial cells alignment and proliferation [6,7]. The ASC plasticity to model blood vessels and to respond to metabolic changes, depends on the acquisition of a smooth muscle cell phenotype which enhances contractility when in contact with endothelial cells [8,9]. In addition, endothelial cells morphogenesis is enhanced by secretion of fibronectin and collagens which in turn allow angiogenesis during either tissue repair or in pathological conditions [10,11]. Furthermore, fibronectins serve multiple roles, most importantly, binding to several other extracellular matrix components to regulate cell adhesion, motility and shape maintenance [12]. Besides, bi-directional interactions between ASC and endothelial cells are sufficient to induce endothelial cells sprouting and extracellular matrix deposition *in vitro*, defining ASC as pre-pericytes that lead vascular morphogenesis processes *in vitro* [13].

However, the temporal dynamics of ASC driven vasculogenesis in three- dimensional microenvironments has not been fully examined. Moreover, cell culture approaches to elucidate vascularization processes *in vitro* and reliably translate findings to *in vivo* situations requires new strategies [14].

In this study we hypothesized that ASC guide endothelial cells to form interconnected structures similar to capillaries. This morphological event was followed in real-time and the extracellular matrix deposition-dependence of the process was observed. Therefore, ASC extracellular matrix production and spatial distribution were analyzed in a three-dimensional microenvironment.

Materials and Methods

Primary cell isolation and cultures

ASC were isolated from lipoaspirates as described previously [33]. Anonymously donated samples were obtained with informed consent as approved by the ethical board of the University Medical Center Groningen following the guidelines for 'waste material'. Propagation of ASC was in DMEM (Dulbecco's modified medium, BioWhittaker Walkersville, MD), 10% not heat inactivated fetal bovine serum (FBS, Thermo Scientific, Helmel Hempstead, UK), 1% l-Glutamine, 1% Penicillin/Streptomycin (Invitrogen, Carlsbad, CA); which was changed for endothelial cells medium (ECM, RPMI-1640 (Lonza Biowhittaker Verviers, Belgium), 10% heat inactivated FBS, 1% l-Glutamine, 1% Penicillin/Streptomycin, 2 mM L-glutamine (Lonza Biowhittaker Verviers, Belgium), 5U/ml heparin (Leo Pharma, The Netherlands) and 5µg/ml of EC growth factor) prior to coculture experiments. Human umbilical vein endothelial cells (HUVEC) were obtained from Lonza (Breda, The Netherlands) and the Endothelial Cell Facility of University Medical Center Groningen, The Netherlands. HUVEC were cultured on gelatin-coated tissue culture polystyrene (TCPS). Porcine retinal endothelial cells (PREC) were isolated from retinas of porcine eyes purchased at the local slaughter house. The protocol was adapted from that described for retinal bovine endothelial cells isolation [16]. Upon receipt the eyes were briefly immersed in 70% ethanol for sterilization purposes. The retinas were harvested from the eyes (approx. 80 eyes per isolation) and washed in DMEM. Subsequently, the retinas were minced in small pieces and incubated with an enzyme cocktail: collagenase type 4 (500µg/ml, Thermo Fisher Scientific, MA USA), DNase (200µg/ml, Roche Diagnostic, Mannheim, Germany) and pronase E (200µg/ml, Roche Diagnostic, Mannheim, Germany) at 37°C for 30min. The digested retinas were filtered through a 60µm mesh nylon filter and the cell

homogenate seeded on gelatin coated plates in DMEM (BioWhittaker Walkersville, MD): 10% fetal bovine serum (FBS), 1% l-Glutamine, 1% P/S. Cells' medium was refreshed every three days. ASC and HUVEC were used between passage 3 and 5. PREC passaged twice were used for downstream applications.

3D printed scaffold design and cells culturing

3D scaffolds were printed with a commercially available 3D printer (Reprap Prusa i3, Anet 3D, China). Biodegradable material, polylactic acid (PLA), was used to print the scaffolds. 3D scaffolds were designed with SketchUp 2016 software. Three-dimensional cocultures were achieved by embedding ASC in combination with either HUVEC or PREC (1×10^5 ASC and 2×10^5 HUVEC or PREC, ratio 1:2) in 100µl of growth factor reduced matrigel® (Corning, New York, USA) accommodated in 3D printed scaffolds (volume: $60mm^3$). ASC and HUVEC were cultured in RPMI, whereas ASC and PREC were cultured in DMEM. Cells in this system were cultured between 3 days and 23 days.

The files of the design and printing can be found at the following link: https://1drv.ms/f/s!AvBi8hGnai5CiHZQIqNuWdN57yzw

Immunostaining

Both scaffolds and sections were fixed in 4% paraformaldehyde in PBS for 30min. Subsequently, cells were permeabilized with 1% BSA and 0.5% Triton-X100 in PBS at room temperature for 1h at 4°C. After PBS washes, primary antibodies were incubated overnight: mouse-anti-human-CD31, PECAM-1 (1:100, Dako, Glostrup, Denmark), rabbit-anti-porcine-PECAM1 (ab28364, Abcam, UK), rabbit-anti-human fibronectin (ab6584, Abcam, UK), F-actin (Alexa Fluor 488 conjugated, ThermoFisher scientific, Odessa, TX), rabbit-anti-human SM22 alpha (ab14106, Abcam, UK). Samples were washed with PBS

and incubated with the fluorescein-conjugated-donkey-anti-mouse-IgG (1:500, Jackson Immunoresearch, UK) and to fluorescein-conjugated-goat-anti-rabbit IgG (1:500, Jackson Immunoresearch, UK) in PBS containing 4',6-diamino-2-phenylindole (DAPI). For colocalization staining in 3D, ASC were CM-DiI-labeled (Thermo Fisher Scientific, Vybrant® CM-DiI red Molecular Probes, Sanbio, Uden, the Netherlands), whereas HUVEC were stained for CD31, PECAM1. Confocal microscope (Leica SP8) was used to acquire z-stack images at 20x, 40x and 63x. Post-processing for imaging was achieved using ImageJ software [17]. Three-dimensional vessel network formations (VNF) were reconstructed using imageJ 3D viewer plugin.

Time-lapse acquisition

3D scaffolds with embedded cocultured cells were placed in a Petri dish (350/15mm) containing 2ml of medium. Cells were labeled with mito tracker (green M7514, red M22426, Molecular probes, Eugene, Oregon, US). Solamere nipkow confocal live cell imaging system was used to acquire time-lapse images. Single particle tracking was achieved using TrackMate (Fiji plugin) [18].

Statistical analysis

All data are presented as a mean of the standard error of the mean and were analyzed using GraphPad Prism 5 (GraphPad Software Inc.). Statistical significance was determined using one-way ANOVA analysis. Values of $p<0.05$ were considered statistically significant.

Results

ASC double role: structure and guidance of endothelial cells

The series of events that underlie the vasculogenic capacity of ASC depend on the extracellular matrix arrangement and cellular sensing of the microenvironment. Understanding the ASC spatial distribution and extracellular matrix deposition, as well as endothelial cells morphogenesis are indispensable to place in context cellular metabolism in health and diseases. In this study, co-cultured ASC and HUVEC, enclosed in matrigel® poured in 3D printed PLA scaffolds, interacted to form aggregates of variable diameter (20-50µm) from which, cells sprouted in all spatial directions (Figure 1A). The boundaries of the scaffold provided anchorage points for the cells (Figure 1A). We have previously shown HUVEC are unable to cross-talk and undergo 3D morphogenesis, in the absence of ASC [19]. DiI labeled ASC enabled the identification of a fraction of cells which localized in pericytic/perivascular positions, specifically ASC surrounded EC aggregates (Figure 1B). The rate of interaction between ASC and EC varied between ASC donors. However, juxtacrine interactions caused HUVEC to aggregate and formed an interconnected network by day 10 for all donors (representative image Figure 1A). Transgelin and fibronectin were detected at day 4 in the coculture of ASC and HUVEC (supplementary video 1). ASC expressing transgelin were found in close association with HUVEC expressing the adhesion molecule PECAM-1 (Figure 1C, left and supplementary video 2). ASC expressing transgelin were also observed when co-cultured with PREC (Porcine retinal endothelial cells) (Figure 1C, right). Fibronectin was expressed ubiquitously throughout the gel forming a network of interconnected fibers (Figure 1C, middle). DAPI staining of cell nuclei and the auto-fluorescence signal from the matrigel® revealed interconnected cavities had formed with a diameter of ~20µm (Figure 1D, left, white arrows). However, few cells (F-actin, Fig. 1D, middle

and right panels) had entered these cavities. Three- dimensional reconstructions of ASC and HUVEC networks after 10 days of coculture showed dense fibronectin deposition in the vicinity of the scaffold wall (Figure 1E, scaffold wall in green (autofluorescence)). Fibronectin was deposited from the scaffold wall inward, whilst the HUVEC network had formed adjacent to the fibronectin layer. The HUVEC network contained ~80 cells in a space of 250µm^3 spanning a length of ~400µm (Figure 1F). There was an average of 200 cells in a volume of 250µm^3 analyzed in four different scaffolds (Figure 1G).

Time-lapse fluorescence microscopy enabled the real-time tracking of mito-tracker labeled cells within the 3D scaffolds. Importantly, ASC and HUVEC could be discriminated based on their mitochondria (labeled with mito tracker, red and green respectively) and therefore the viability of both cell types was verified. First, an aggregate of 5 cells, either HUVEC or ASC, was followed over time (Figure 2A). One HUVEC displayed several cytomembrane extensions of 40µm length, reaching out towards other HUVEC. This first stage of assembly took place in the first 36h of co-culture. However, HUVEC also aggregated in greater numbers (~20 cells), and the presence of HUVEC labeled mitochondria confirmed survival and activity of these cells (Figure 2B and supplementary video 3, HUVEC aggregates in green). Following endothelial cells aggregation, sprouting occurred between 7 and 9 hours. As showed in figure 2C, the process of sprouting was polarized at one position relative to the HUVEC aggregation (white square and arrow indicate direction, figure 2C). ASC surrounded the HUVEC aggregate, suggesting a role for the ASC in promoting sprouting by oscillatory movements (supplementary video 4). Concomitantly, endothelial cells which did not participate in the aggregation were also present, shown in figure 2D. These non-participating cells stretched cytomembrane extensions up to 100µm to reach out and connect with endothelial cell aggregations. Finally, further endothelial cells were

observed to contact leading endothelial cells through cytoplasmic extensions in the direction of aggregated cells (Figure 2E, endothelial cells' mitochondria in green)

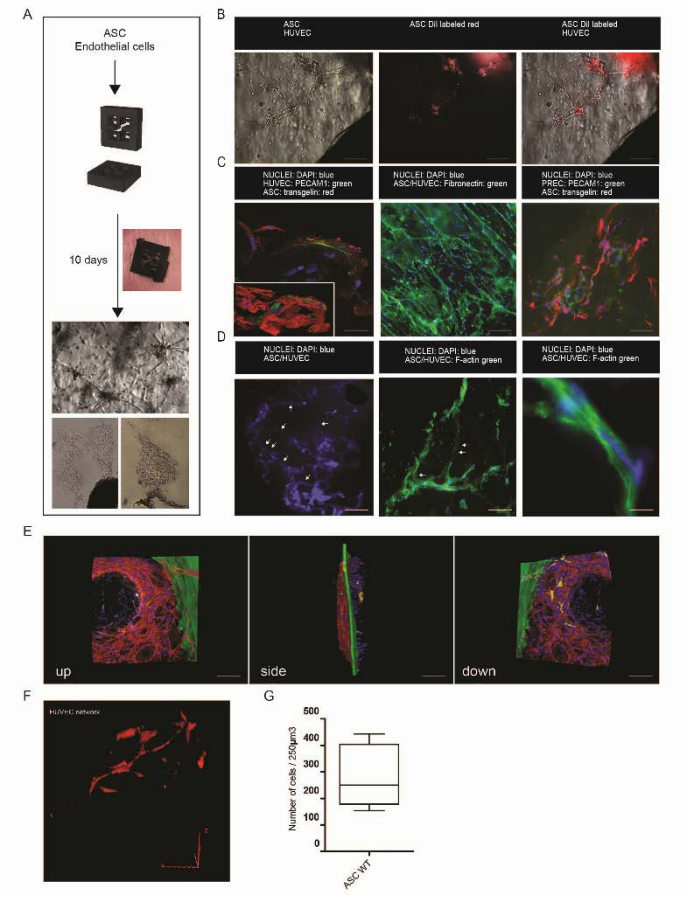

Figure 1. Adipose stromal cells (ASC) juxtacrine communication and extracellular matrix guide endothelial cells assembly in confined microenvironments. ASC were embedded in matrigel for 10 days with either HUVEC or porcine retina endothelial cells (PREC). Several interconnected cell aggregates are depicted in the middle panel. Left and right panels show cell aggregates' contact points to the scaffold (A). ASC and endothelial cells tube formation (B-left). DiI labeled ASC (red) enclosed endothelial cells aggregates (B-middle). Merged endothelial tube formation and DiI labeled ASC (B-right). During tube formation, ASC expressed transgelin contractile proteins while HUVEC expressed PECAM-1 (C-left). Fibronectin deposition as to form an interconnected net in the presence of ASC/HUVEC (C-middle). ASC, expressing marker transgelin and PREC expressing marker PECAM-1 (C-right). Longitudinal section showed interconnected cavities formed by ASC extracellular matrix degradation with a diameter of ~20µm (D-left, DAPI and auto-fluorescence). Cytoskeletal protein F-actin was expressed by co-cultured ASC and HUVEC (D-middle and –right). Fibronectin deposition and organization visualized after z-stack reconstruction (E, field of view ~500x500µm). HUVEC network extrapolated from co-cultured with ASC (F). (G) Number of cells relative to field of view ~500x500µm, h: ~50 µm. Scale bars: (A-middle) 100µm, (A-left) 50µm, (A-right) 50µm (B) 200µm, (C-left) 20µm, (C-right) 100µm, (C-right) 100µm, (D-left) 50µm, (D-middle) 50µm, (D-right) 10µm, (E) 50µm, (F) 50µm.

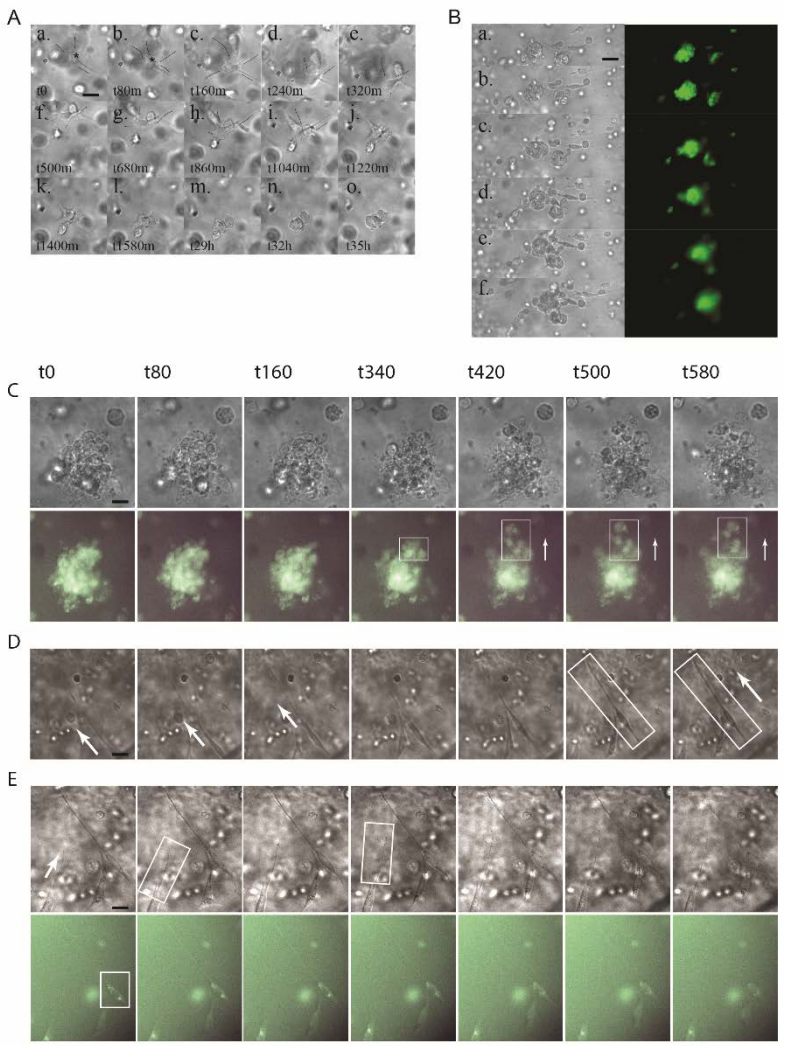

Figure 2. ASC guide endothelial cells sprouting. HUVEC stained mitochondria (mito-tracker green) were followed in time. From one HUVEC several protrusions interacted with other HUVEC. After 35 hours an aggregate of HUVEC was formed (A). HUVEC aggregates and single HUVEC interacted to form aggregates of greater size (B). HUVEC sprouted from aggregates between 420 to 580 minutes (C), (white rectangle and arrow for direction). Not all HUVEC participated in aggregates. Single HUVEC contacted aggregates by extending up to 100µm (D). More single HUVEC contacted one another as to form network (E), mitochondria identifying HUVEC, (green). Scale bars: (A) 10µm, (B) 40µm, (C) 20µm, (D) 20µm, (E) 20µm.

Cellular speed variance in long term cultures

As shown previously, ASC cocultured with either HUVEC or PREC generated an interconnected vascular network throughout the scaffold within 10 days (Figure 1). This vascular-like network was maintained for over 30 days, while structural differences were related to the spatial organization of cells in sinusoids being 10-50µm bigger in diameter when ASC/HUVEC were compared with ASC/PREC (data not shown). DiI labeled ASC were closely aligned with PREC (PECAM-1, green). ASC/PREC co-localizations were observed after three weeks of coculture (Figure 3A). In this experiment 3D cocultures of ASC and PREC was analyzed using TrackMate for cellular dynamism (Figure 3B, C). Tracking of cells showed that the majority of cells within the aggregate moved forward up to 15 µm per 60min. Only 2 to 3 cells within the aggregate moved at a faster rate of 21 µm in 30 min, suggesting that these cells represent endothelial cells which were preparing to sprout from the aggregates (Figure 3D). Calculation of the mean velocity showed that the aggregate of cells moved and oscillated at a rate of 0 to 2 µm per frame (30 min). Faster cells that is, sprouting endothelial cells, moved at a rate of 2 to 4 µm per frame (30 min) (Figure 3E).

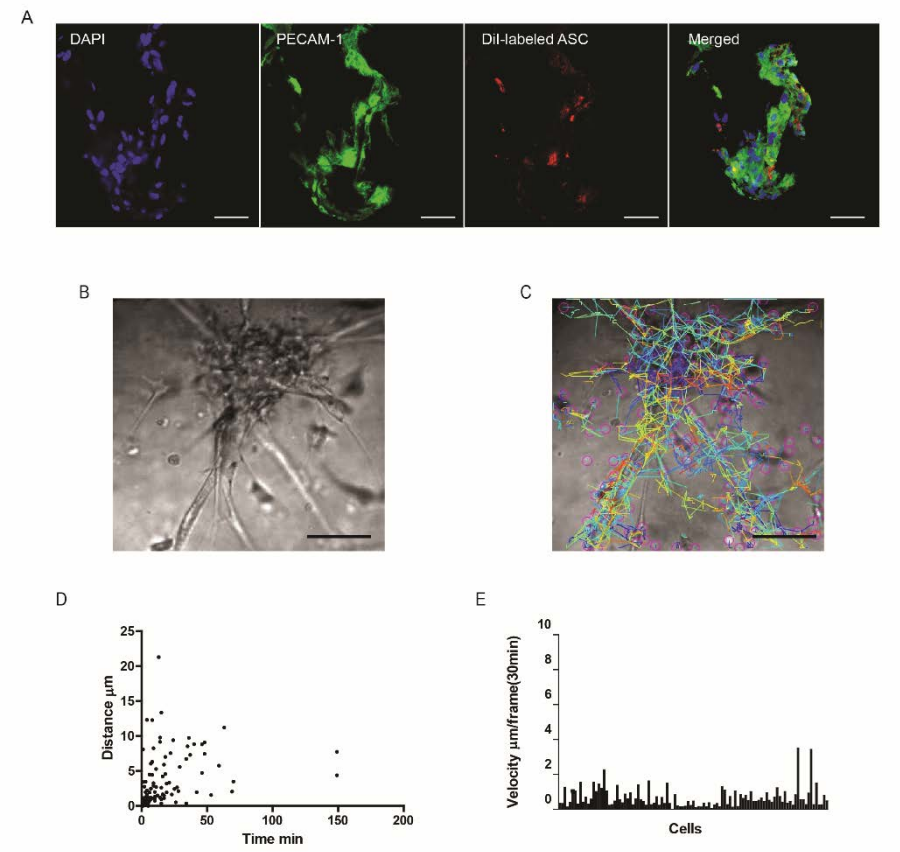

Figure 3. Long term coculture retains cellular contractions and movements between aggregates. ASC and PREC were co-cultured for over 23 days. ASC DiI-labeled (red) integrated in PREC network (PECAM-1, green) (A). Time-lapse microscopy analysis of one of the aggregates with endothelial cells protrusions (B). Plug-in TrackMate (imageJ) was used to path cells' trajectories (C). Cells' trajectories represented as distance covered (µm) relative to time (minutes) (D). Velocity of cells was calculated in µm/frame (30min) (E). Scale bars: 20 µm.

Diabetic ASC fail to support formation of 3D networks by endothelial cells

In the previous sections, we described the morphological events that led to vascular-like network formation in a coculture of ASC and endothelial cells. This was achieved in a confined 3D microenvironment comprising a basal membrane-derived matrix (Matrigel®). This platform allows the reiteration of important components of disturbed vasculogenesis such as in diabetic wound healing or in diabetic retinopathy. Therefore, we assessed the capacity of ASC from diabetic donors to support vasculogenesis.

Diabetic ASC (D-ASC) partially lost the capacity to support endothelial cell tube formation. Furthermore, we also investigated how ASC supported and adapted to primary retinal endothelial cells. These characteristics were examined by measuring fibronectin deposition, PECAM-1 expression as well as the cell's spatial distribution in three-dimensions. In cocultured ASC with HUVEC fibronectin was deposited throughout the whole area analyzed (measured as mean fluorescence intensity in 250µm^3, 6.539±0.145), while D-ASC cocultured with HUVEC and D-ASC cocultured with PREC showed decreased fibronectin deposition (2.361±0.110; 2.316±0.056) respectively (Figure 4A). Similarly, PECAM-1 expression was higher in HUVEC cocultured with ASC (2.496±0.028), while decreased PECAM-1 expression was detected in both HUVEC cocultured with D/ASC and PREC cocultured with ASC (0.940±0.011; 1.240±0.031) respectively (Figure 4B). Figure 4C shows fibronectin and PECAM1 expression and spatial distribution in ASC/HUVEC, D-ASC/HUVEC and, ASC/PREC respectively. Finally, an interconnected tube-like network was observed when ASC were cocultured with HUVEC (Figure 4D). In this representation, ASC illustrated by nuclear staining in the absence of PECAM1 expression were counted and classified by

their position. In ASC/HUVEC there were about 200 cells counted and about half of these were detected in a perivascular location in the 3D space.

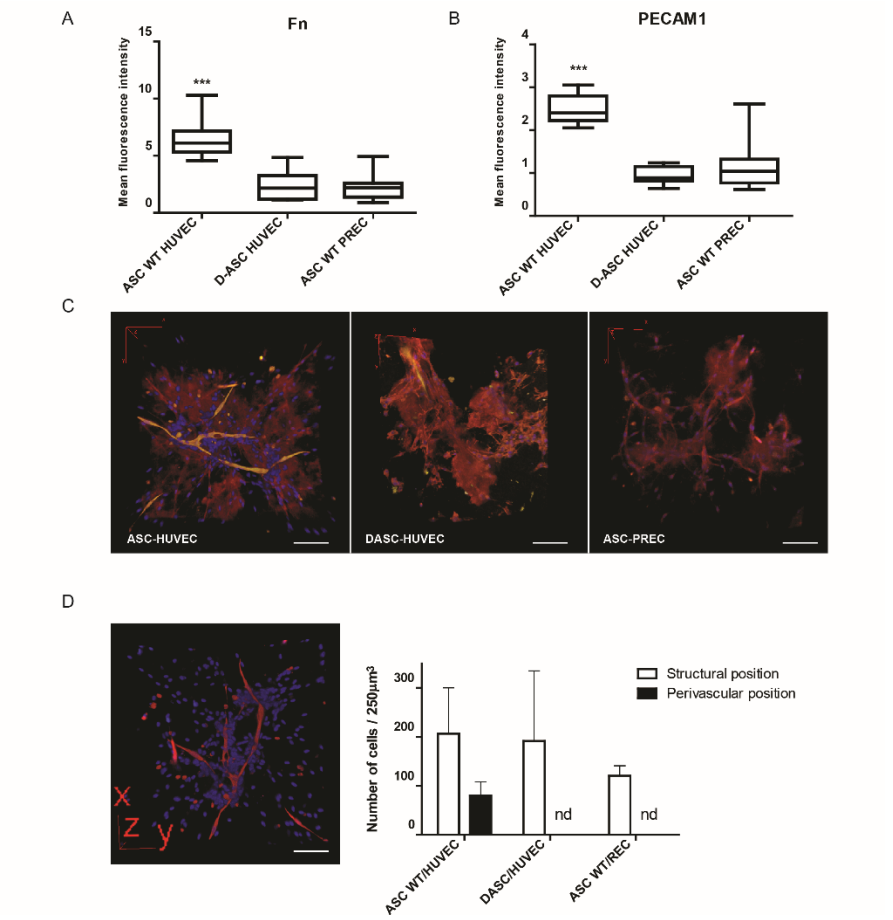

Figure 4. Diabetic ASC do not homogeneously secrete fibronectin and endothelial tube formation is impaired. Three-dimensional characterization of fibronectin and PECAM-1 expression in ASC/HUVEC, diabetic ASC/HUVEC and ASC/PREC. Cells embedded in matrigel were placed in the scaffolds. Cross-sections of 100 µm were stained after 10 days of culturing (A). Fibronectin and PECAM-1 were deposited in higher amount in co-cultured ASC and HUVEC, while diabetic ASC/HUVEC and ASC/PREC had similar expression of both fibronectin and PECAM-1 (A, B and C, ***, $p \leq 0.001$, one-way ANOVA). ASC and HUVEC three-dimensional reconstruction with HUVEC forming network (~100 cells) and static HUVEC (~80 cells). (D). Acquisitions size: ~500x500 µm, h: ~80 µm. Scale bars: 100µm.

Discussion

Understanding the role of adipose tissue-derived stromal cells functional heterogeneity in promoting endothelial cell organization in a three-dimensional confined microenvironment was the main aim of this study. The ASC were found to elicit a structurally important function by remodeling matrigel® and, concomitantly, promoting tube formation by endothelial cells. In this model, ASC facilitated two basic processes: 1) preparing extracellular matrix for endothelial cells invasion and 2) surrounding endothelial cell aggregates to apply contractile pressure and promote endothelial cells' sprouting. Endothelial cells formed several aggregates of variable sizes which connected to form tubes. The cellular aggregates and tubes preserved dynamism over the long term. Sprouting endothelial cells moved at a higher speed when compared to endothelial cells within the aggregates. This behavior was observed in both HUVEC and PREC. In striking contrast, tube formation and fibronectin secretion were impaired when diabetic ASC were used.

Three-dimensional microenvironments are fundamental to investigate physiological and developmental processes to reduce the gap between *in vitro* and *in vivo* studies [20]. With these systems it is possible to recapitulate the intricate relationship existing between cells and extracellular matrix with the direct advantage of observing, measuring and manipulating cell morphogenesis, proliferation, differentiation and tissue structure [21]. The system developed in this study, allowed ASC and endothelial cells to be observed in a confined microenvironment which enabled the following of vessel morphogenesis and structural organization in time [22]. Cellular migration, assembly and organization was highly heterogeneous and, cellular behavior in space and time notably differ among single cells, aggregates and cells protruding from

the aggregates [23]. Extracellular matrix plays an important role in regulating cell contraction, migration, shape and survival [24,25]. We demonstrated that endothelial cells organization and assembly was under direct ASC juxtacrine control and through extracellular matrix production. Endothelial cells aggregates were sprouting under the contractile pressure of ASC, while fibronectin homogeneously expressed ascertained the maintenance of the tissue turgor [26].

The three-dimensional culture systems also offered a platform for studying cell processes during diseases [27]. Fibronectin is important for cellular contraction and organization during tissue repair and morphogenesis [28]. Importantly, we showed that fibronectin deposition from diabetic ASC was less organized, compared to the non-diseased ASC, and did not support capillary-like tube formation by endothelial cells. Organogenesis depends on self-assembly and cellular organization; several models have been proposed and are progressively improving our understanding of human development and diseases [29]. In this study, ASC vasculogenesis potential was further explored and, time lapse microscopy in combination with three-dimensional culturing revealed the cellular processes underlying endothelial cells tube formation were dependent upon extracellular matrix deposition [30]. Moreover, three-dimensional imaging reconstruction is a powerful tool to analyze cellular heterogeneity [31]. ASC initially manipulate the extracellular matrix microenvironment to allow endothelial cells sprouting. Secondly, deposit extracellular matrix to maintain a stable structure. ASC in the same population induce sprouting of endothelial cells aggregates. In conclusion, the three- dimensional culturing approach described in this study is a powerful but simple method to extrapolate important information about cellular dynamism [32]. Implementation with other cellular populations, protein tracking and drug testing, has the potential to exponentially enhance our

understanding of cellular processes *in vitro* and safely translate findings to *in vivo* models.

Acknowledgements

The authors would like to thank Klaas Sjollema (UMCG Microscopy and Imaging Center (UMIC)) for kindly assisting with time-lapse image acquisition. JKB was supported by the University of Groningen and European Union co-Funded Rosalind Franklin Fellowship. VT: Concept and design, data collection, analysis and interpretation, manuscript writing, final approval. GRL: Revision of manuscript, final approval. JKB: Revision of manuscript, final approval of manuscript. HPH: Financial support, revision of manuscript, final approval of manuscript. MCH: Revision of manuscript, financial support, final approval.

Disclosure of potential conflicts of interest

The authors declare no potential conflicts of interest.

References

1. Bourin P, Bunnell BA, Casteilla L, et al (2013) Stromal cells from the adipose tissue-derived stromal vascular fraction and culture expanded adipose tissue-derived stromal/stem cells: a joint statement of the International Federation for Adipose Therapeutics and Science (IFATS) and the International So. Cytotherapy 15:641–648.

2. da Silva Meirelles L, de Deus Wagatsuma VM, Malta TM, et al (2016) The gene expression profile of non-cultured, highly purified human adipose tissue pericytes: Transcriptomic evidence that pericytes are stem cells in human adipose tissue. Exp Cell Res 349:239–254.

3. Rumman M, Dhawan J, Kassem M (2015) Concise Review: Quiescence in Adult Stem Cells: Biological Significance and Relevance to Tissue Regeneration. Stem Cells 33:2903–2912.

4. Cao Y (2010) Adipose tissue angiogenesis as a therapeutic target for obesity and metabolic diseases. Nat Rev Drug Discov 9:107–115.

5. Lijnen HR (2008) Angiogenesis and obesity. Cardiovasc Res 78:286–293.

6. Merfeld-Clauss S, Lupov IP, Lu H, et al (2014) Adipose stromal cells differentiate along a smooth muscle lineage pathway upon endothelial cell contact via induction of activin A. Circ Res 115:800–809.

7. Przybyt E, Van Luyn MJA, Harmsen MC (2015) Extracellular matrix components of adipose derived stromal cells promote alignment, organization, and maturation of cardiomyocytes in vitro. J Biomed Mater Res - Part A 103:1840–1848.

8. Merfeld-Clauss S, Lupov IP, Lu H, et al (2015) Adipose Stromal Cell Contact with Endothelial Cells Results in Loss of Complementary Vasculogenic Activity Mediated by Induction of Activin A. Stem Cells 33:3039–3051.

9. Wang C, Yin S, Cen L, et al (2010) Differentiation of adipose-derived stem cells into contractile smooth muscle cells induced by transforming growth factor-beta1 and bone morphogenetic protein-4. Tissue Eng Part A 16:1201–1213.

10. Stoffels JMJ, Zhao C, Baron W (2013) Fibronectin in tissue regeneration: Timely disassembly of the scaffold is necessary to complete the build. Cell Mol Life Sci 70:4243–4253.

11. Paulsson M (1992) Basement membrane proteins: structure, assembly, and cellular interactions. Crit Rev Biochem Mol Biol 27:93–127.

12. Pankov R, Yamada KM (2002) Fibronectin at a glance. J Cell Sci 115:3861–3863.

13. Merfeld-Clauss S, Gollahalli N, March KL, Traktuev DO (2010) Adipose Tissue Progenitor Cells Directly Interact with Endothelial Cells to Induce Vascular Network Formation. Tissue Eng Part A 16:2953–2966.

14. Zhang X, Bendeck MP, Simmons CA, Santerre JP (2017) Deriving vascular smooth muscle cells from mesenchymal stromal cells: Evolving differentiation strategies and current understanding of their mechanisms. Biomaterials 145:9–22.

15. Zuk PA, Zhu M, Ashjian P, et al (2002) Human adipose tissue is a source of multipotent stem cells. Mol Biol Cell 13:4279–4295.

16. Banumathi E, Haribalaganesh R, Babu SSP, et al (2009) High-yielding enzymatic method for isolation and culture of microvascular endothelial cells from bovine retinal blood vessels. Microvasc Res 77:377–381.

17. Schneider CA, Rasband WS, Eliceiri KW (2012) NIH Image to ImageJ: 25 years of image analysis. Nat Methods 9:671–675.

18. Tinevez J-Y, Perry N, Schindelin J, et al (2017) TrackMate: An open and extensible platform for single-particle tracking. Methods 115:80–90.

19. Terlizzi V, Kolibabka M, Burgess JK, et al (2017) The Pericytic Phenotype of Adipose Tissue-derived Stromal Cells is Promoted by NOTCH2. Stem Cells. 2018 Feb;36(2):240-251.

20. Sala A, Hanseler P, Ranga A, et al (2011) Engineering 3D cell instructive microenvironments by rational assembly of artificial extracellular matrices and cell patterning. Integr Biol 3:1102–1111.

21. Rosso F, Giordano A, Barbarisi M, Barbarisi A (2004) From Cell-ECM Interactions to Tissue Engineering. J Cell Physiol 199:174–180.

22. Votteler M, Kluger PJ, Walles H, Schenke-Layland K (2010) Stem cell microenvironments--unveiling the secret of how stem cell fate is defined. Macromol Biosci 10:1302–1315.

23. Sharma Y, Vargas DA, Pegoraro AF, et al (2015) Collective motion of mammalian cell cohorts in 3D. Integr Biol 7:1526–1533 .

24. Adams JC (1997) Characterization of cell-matrix adhesion requirements for the formation of fascin microspikes. Mol Biol Cell 8:2345–2363

25. Sethi KK, Yannas I V, Mudera V, et al (2002) Evidence for sequential utilization of fibronectin, vitronectin, and collagen during fibroblast-mediated collagen contraction. Wound Repair Regen 10:397–408

26. Couchman JR, Rees DA (1979) The behaviour of fibroblasts migrating from chick heart explants: changes in adhesion, locomotion and growth, and in the distribution of actomyosin and fibronectin. J Cell Sci 39:149–165

27. Clevers H (2016) Modeling Development and Disease with Organoids. Cell 165:1586–1597.

28. Meckmongkol TT, Harmon R, McKeown-Longo P, Van De Water L (2007) The fibronectin synergy site modulates TGF-beta-dependent fibroblast contraction. Biochem Biophys Res Commun 360:709–714.

29. Lancaster MA, Knoblich JA (2014) Organogenesis in a dish: Modeling development and disease using organoid technologies. Science (80-) 345:1247125–1247125.

30. Kanno S, Fukuda Y (1994) Fibronectin and tenascin in rat tracheal wound healing and their relation to cell proliferation. Pathol Int 44:96–106

31. MacLean AL, Smith MA, Liepe J, et al (2017) Single Cell Phenotyping Reveals Heterogeneity Among Hematopoietic Stem Cells Following Infection. Stem Cells 35:2292–2304 .

32. Driscoll MK, Danuser G (2015) Quantifying Modes of 3D Cell Migration. Trends Cell Biol 25:749–759 .

Supplementary videos are available in the online version of this thesis

Supplementary video 1. Building the vascular network. ASC deposit fibronectin (red) while HUVEC (PECAM-1, green) begin to assemble in to tube-like network. Time point: day 4.

Supplementary video 2. Wrapping and supporting the vessels. ASC (transgelin, red) wrap and support HUVEC (PECAM-1, green) during vasculogenesis. Time point: day 4.

Supplementary video 3. Endothelial cells team work. Time-lapse microscopy was used to follow cells. HUVEC aggregates merging as to form bigger aggregates in size. Time: 22 hours.

Supplementary video 4. ASC oscillation induced endothelial cells sprouting. Time-lapse confocal microscopy and mitochondria labeled cells were followed. ASC (red) oscillatory movements induced HUVEC (green) to sprout. Time: 35 hours

Video files can be found at the following link:

https://1drv.ms/f/s!AvBi8hGnai5CiHFwWJ2mkAIX2FSN